Available online at www.sciencedirect.com

ScienceDirect

Energy Procedia 126 (201709) 337–344

Energy Procedia

www.elsevier.com/locate/procedia

72nd Conference of the Italian Thermal Machines Engineering Association, ATI2017, 6-8 September 2017, Lecce, Italy

A two-dimensional model of a solid-state regenerator based on combined electrocaloric-elastocaloric effect

Ciro Aprea[a], Adriana Greco[b], Angelo Maiorino[a], Claudia Masselli[a,*]

[a]DIIN University of Salerno, Via Giovanni Paolo II 132, Fisciano (SA) 84084, Italy
[b]DII University of Naples Federico II, P.le Tecchio 80, Napoli 80125, Italy

Abstract

Solid-state refrigeration technologies are considered nowadays emerging alternative to vapor compression refrigeration. In this paper is introduced a two-dimensional model of solid-state refrigerator, which employs materials experiencing a combined electrocaloric-elastocaloric effect and it operates at room temperature. A numerical investigation is performed to explore the energetic performance of the refrigerators. The results reveal that $PbTiO_3$ as elastocaloric refrigerant confers the best performances in terms of COP; the highest cooling power estimated are proper of combined elastocaloric-electrocaloric effect, with increments around +65% than employing $PbTiO_3$ in single electrocaloric/elastocaloric refrigeration, on equal operative conditions.

Peer-review under responsibility of the scientific committee of the 72nd Conference of the Italian Thermal Machines Engineering Association

Keywords: electrocaloric refrigeration; elastocaloric refrigeration; solid-state refrigeration; multicaloric effect; two-dimensional model;

1. Introduction

On the world stage, it has been estimated that refrigeration and air conditioning provoke 17% of energy consumption. The technology main responsible of such data is vapour compression (VC) since most of the refrigeration and air conditioning systems is based on. The refrigerants employed in VC have been multiple: from

* Corresponding author. Tel.: +39-089-964315; fax: +39-089-964037.
E-mail address: cmasselli@unisa.it

1876-6102
Peer-review under responsibility of the scientific committee of the 72nd Conference of the Italian Thermal Machines Engineering Association
10.1016/j.egypro.2017.08.225

CFCs and HCFCs, interdicted by the Montreal Protocol [1] because of their capability to deplete the stratospheric ozone level (ODP, Ozone Depletion Potential), onward HFCs, without ODP but with a significant GWP (Global Warming Potential), whom are actually the only fluorinated fluids avoided. As a matter of fact, even if nowadays the contribution consists of 1% of all over the world greenhouse gases ones, HFC's emission are growing by 8-9% annually [2].

Nomenclature

C	specific heat, [J kg^{-1} K^{-1}]
COP	Coefficient of Performance
E	electric field, [V m^{-1}]
H	magnetic field [A m^{-2}]
k	thermal conductivity, [W m^{-1} K^{-1}]
m	mass flow rate, [kg s^{-1}]
M	magnetization, [A m]
p	pressure, [Pa]
P	polarization, [C m^{-2}]
Q	thermal energy, [J]
Q	thermal power, [W]
Q	heat source term, [W m^{-3}]
S	entropy, [J K^{-1}]
s	specific entropy, [J kg^{-1} K^{-1}]
T	temperature, [K]
t	time, [s]
u	longitudinal fluid velocity, [m s^{-1}]
V	volume, [m^3]
v	orthogonal fluid velocity, [m s^{-1}]
v	specific volume, [m^3 kg^{-1}]
W	work, [J]
X	conjugate field
x	longitudinal spatial coordinate, [m]
Y	applied driving field
y	orthogonal spatial coordinate, [m]
Δ	finite difference
ε	uniaxial strain
η	isentropic efficiency
μ	viscosity, [Pa s]
$\mu 0$	vacuum magnetic permeability, [T m A^{-1}]
ν	cinematic viscosity, [m^2 s^{-1}]
ρ	density, [kg m^{-3}]
σ	uniaxial stress, [Pa]
τ	period of each phase of the cycle, [s]

With the Kyoto Protocol [3] and therefore with the consequent national laws and regulations, more stringent goals in the reduction of greenhouse gas emissions have been established, all having as common denominator the HFC consumption's phasing out [4-5]. Human activities have increased the energy consumption in buildings [6-11], because of the growing HVAC employment, environmental pollution and the concentration of greenhouse gases in the atmosphere. This resulted in a substantial warming of earth surface and atmosphere that adversely affected the natural ecosystem. Therefore, the attention now is paid to the non-vapor-compression technologies for refrigeration and air conditioning.

Solid-state refrigeration technologies are considered nowadays emerging alternative to vapor compression refrigeration. They are gaining more and more attentions, due to their potential in being performing and ecological methodologies. Among them electrocaloric [12,13] and elastocaloric cooling [14], seems to be really promising since they could constitute a real chance to overcome vapor compression refrigeration limits. As a matter of fact, solid state refrigerations could confer energy efficiency, theoretically, 50-60% higher than vapor compression [15].

Electrocaloric and elastocaloric cooling are based respectively upon electrocaloric effect (ECE) and elastocaloric effect (eCE): two caloric effect detected in ferroelectric/ferroelastic materials where, a change of an external (electric/structural) field in adiabatic condition provokes a variation in the material's temperature. Such phenomena belong to the more general class of caloric effects, manifesting themselves in caloric materials. Caloric materials show reversible thermal changes, known as caloric effects, that are due to changes in applied driving field. These thermal changes are parameterized via isothermal entropy change ΔS and adiabatic temperature change ΔT_{ad}, defined respectively as:

$$\Delta S = \int_{Y_0}^{Y_1} \left(\frac{\partial X}{\partial T}\right)_Y dY \tag{1}$$

$$\Delta T_{ad} = -\int_{Y_0}^{Y_1} \frac{T}{C} \left(\frac{\partial X}{\partial T}\right)_Y dY \tag{2}$$

By changing the driving field a variation of the conjugate one is registered. If the variation has induced isothermally, the caloric effect is quantified by (1); dually if the field changes adiabatically, ΔT_{ad} constitutes a measure of the phenomenon. Caloric materials and caloric effects are named according to the sign of the caloric effect and to the nature of the applied driving field, as described below. In the first place, conventional caloric materials show $\Delta S < 0$ and $\Delta T_{ad} > 0$, when the magnitude of the driving field is increased. Inverse caloric materials show $\Delta S > 0$ and $\Delta T_{ad} < 0$, when the magnitude of the driving field is increased [16]. The above expressions quantify the magnetocaloric ($Y = H$ and $X = M$), barocaloric ($Y = -p$ and $X = V$), elastocaloric ($Y = \sigma$ and $X = \varepsilon$) and electrocaloric ($Y = E$ and $X = P$) effects [17]. Consequently, isothermal entropy change ΔS and adiabatic temperature change ΔT_{ad}, with reference to electrocaloric effect, become:

$$\Delta S = \int_{E_0}^{E_1} \left(\frac{\partial P}{\partial T}\right)_E dE \tag{3}$$

$$\Delta T_{ad} = -\int_{E_0}^{E_1} \frac{T}{C} \left(\frac{\partial P}{\partial T}\right)_E dE \tag{4}$$

Dually, with reference to elastocaloric effect, they become as follow:

$$\Delta S = \int_{\sigma_0}^{\sigma_1} \left(\frac{\partial \varepsilon}{\partial T}\right)_\sigma d\sigma \tag{5}$$

$$\Delta T_{ad} = -\int_{\sigma_0}^{\sigma_1} \frac{T}{C} \left(\frac{\partial \varepsilon}{\partial T}\right)_\sigma d\sigma \tag{6}$$

Multicaloric materials can support more than one type of caloric effect. Experimental studies [18] reveal that multicaloric effects would arise if more than one type of caloric effect were driven simultaneously or sequentially in a single sample of caloric material. In this paper is introduced an experimental investigation conducted on a two-dimensional model of solid-state cooler when it employs $PbTiO_3$, a multicaloric material which presents both electrocaloric and elastocaloric effect, in order to explore its energetic performances both when the material only shows electrocaloric or elastocaloric effect alone and when its multicaloric nature takes place.

2. Thermodynamical cycles for electro/elastocaloric refrigeration

Electrocaloric and elastocaloric refrigeration are both reverse Brayton cycle based whom its principle of operation is reported on an S-T diagram shown in Fig. 1(a): there are two adiabatic and two isofield processes. By polarization/stressing (1-2) an increment of the caloric material's temperature is registered. In the stage (2-3) the heat generated, due to caloric effect, is rejected through a heat transfer toward a heat sink. In the stage (3-4), the field is removed and therefore the material cools down thanks to ECE/eCE. In the fourth stage (4-1), the solid-state material, which currently is cold, absorb heat from cold reservoirs and recovers the initial state [19]. An inverse Brayton cycle, referred to electrocaloric/elastocaloric refrigeration, if the caloric material plays both the refrigerating and regenerator role, evolves in Active Electrocaloric/elastocaloric Regenerative cycle (AER/AeR). In AER/AeR cycle a secondary fluid (water) is introduced as a heat transfer vector whom crosses the regenerator.

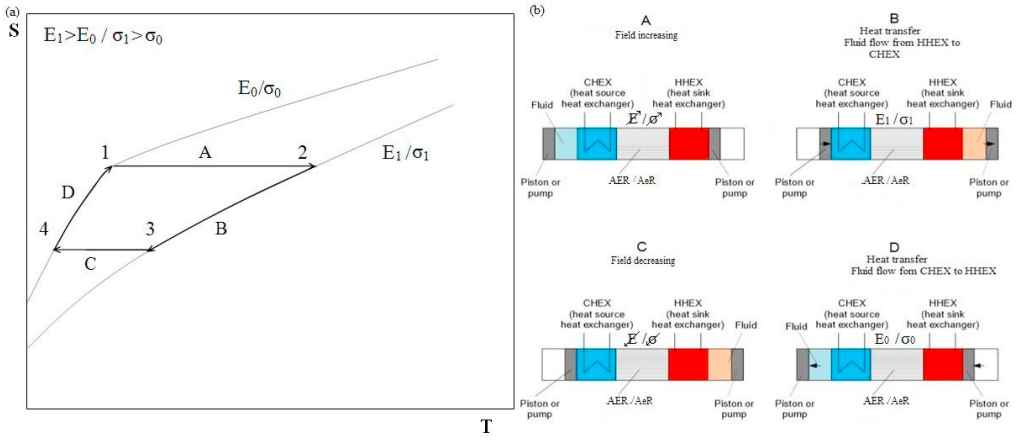

Fig. 1. (a) Inverse Brayton cycle on T-s diagram; (b) The four processes of AER/AeR cycle.

The working principle of AER/AeR cycle is shown in Fig. 1(b). During the field increasing process (A), the electric field/uniaxial stress, applied to the caloric material, is increased until reaching the maximum value (E_1/σ_1) while the fluid is not flowing, causing the increasing of the material's temperature, due to ECE/eCE. In the second stage (B), the field remains constant and the cold fluid crosses the AER/AeR from the cold to the hot side, thus cooling the regenerator and rejecting heat in the external environment through the hot heat exchanger. When in the third stage (C) the field is reduced until reaching the minimum value (E_0/σ_0), while the fluid hasn't any motion, the regenerator sees another decrement in its temperature, thanks to ECE/eCE. As a final stage (D), while the field is absent, the fluid flows across the regenerator from the hot to cold side, cooling itself and then reaching the cold heat exchanger, where it absorbs heat from the latter, producing a cooling load.

3. Model description

In this paper is introduced a two-dimensional model of an active caloric refrigerator. The model is able to reproduces the behavior of an active regenerator in parallel-plate configuration either when the caloric effect is electrocaloric one, either when it is elastocaloric and when it is combined ECE-eCE (multicaloric). Every plate has the same thickness (0.25 mm) and the distance stacked between each other is 0.125 mm, which also corresponds to each fluid channel thickness. The wrapper which contains the regenerator occupies a 20x45 mm^2 area, whom is occupied globally for 60% from the parallel plates made of caloric refrigerant. The simulations have been carried out, bearing in mind of the succeeding reported hypothesis:

- absence of Eddy currents and negligible Joule heating;
- neglecting of heat radiation and thermal hysteresis;

- adiabatic regenerator with infinite heat exchange area.

To describe accurately, the regenerator's behavior by a mathematical model, is appropriate to specify that each of the four AMR/AER processes is modeled by distinct sets of equations. The fluid flow processes are governed by the Navier-Stokes and the solid and fluid energy equations, to be aware of the temperatures and fluid velocity, as follows:

$$\begin{cases} \dfrac{\partial u}{\partial x}+\dfrac{\partial v}{\partial y}=0 \\ \dfrac{\partial u}{\partial t}+u\dfrac{\partial u}{\partial x}+v\dfrac{\partial u}{\partial y}=-\dfrac{1}{\rho_f}\dfrac{\partial p}{\partial x}+\upsilon\left(\dfrac{\partial^2 u}{\partial x^2}+\dfrac{\partial^2 u}{\partial y^2}\right) \\ \dfrac{\partial v}{\partial t}+u\dfrac{\partial v}{\partial x}+v\dfrac{\partial v}{\partial y}=-\dfrac{1}{\rho_f}\dfrac{\partial p}{\partial y}+\upsilon\left(\dfrac{\partial^2 v}{\partial x^2}+\dfrac{\partial^2 v}{\partial y^2}\right) \\ \dfrac{\partial T_f}{\partial t}+u\dfrac{\partial T_f}{\partial x}+v\dfrac{\partial T_f}{\partial y}=\dfrac{k_f}{\rho_f C_f}\left(\dfrac{\partial^2 T_f}{\partial x^2}+\dfrac{\partial^2 T_f}{\partial y^2}\right) \\ \dfrac{\partial T_s}{\partial t}=\dfrac{k_s}{\rho_s C}\left(\dfrac{\partial^2 T_s}{\partial x^2}+\dfrac{\partial^2 T_s}{\partial y^2}\right) \end{cases} \tag{7}$$

where it has been assumed that the fluid is incompressible and laminar and, because of the low mass flow, the viscous dissipation is neglected. Field increasing/decreasing processes are regulated by the energy equations. In the solid energy equation, one can see a heat source term Q, which models the ECE/eCE. It depends on the intensity of the applied external field and it is proportional to ΔT_{ad} as follows:

$$Q = Q(field, T_S) = \frac{\rho_S\, C\,(field, T_S)\,\Delta T_{ad}(field\,, T_S)}{\tau} \tag{8}$$

Q, since is a power density, which is positive during field increasing, negative during field decreasing. Therefore, the equation system is:

$$\begin{cases} \rho_f C_f \dfrac{\partial T_f}{\partial t}=k_f\left(\dfrac{\partial^2 T_f}{\partial x^2}+\dfrac{\partial^2 T_f}{\partial y^2}\right) \\ \rho_s C\dfrac{\partial T_s}{\partial t}=k_s\left(\dfrac{\partial^2 T_s}{\partial x^2}+\dfrac{\partial^2 T_s}{\partial y^2}\right)+Q \end{cases} \tag{9}$$

By an elaboration of experimental data of $\Delta T_{ad}(E/\sigma,T)$ for $PbTiO_3$, available from literature [18], and considering the physical characteristic reported in Table 1, it has been built the functions of $Q(E/\sigma,T)$. The corresponding mathematical expressions of Q for field increasing and field decreasing processes, for ECE, eCE and combined effect, have been obtained through an analytical function finder software.

Table 1. Physical characteristics of $PbTiO_3$.

Material	ρ [kg/m^3]	k [W/mK]	C [J/kgK]
$PbTiO_3$	8000	4	379.5

By the way, the AER/AeR behaviors, have been obtained by solving the mathematical systems (eq. (7) and (9)) that rule AER/AeR cycles, using Finite Element Method. The cycle is conceived as a succession of sequential stages: the initial conditions of one of them are the results of the previous one. Every stage has a period τ which is the same during all the processes of the AER/AeR cycle. The presence of heat exchangers, during fluid flow phases, are obtained applying first order boundary conditions: T_C and T_H, the temperatures of the cold and hot heat exchanger, on the left and right boundary, respectively, of the AER/AeR regenerator. The simulations are done, repeating AER/AeR cycle several times with constant frequency, until reaching the steady state.

4. Numerical investigation

Numerical simulations described in this paper have been performed on $PbTiO_3$ in three distinct cases: when it is employed as a) electrocaloric material for electrocaloric refrigeration; b) elastocaloric material for elastocaloric refrigeration; c) multicaloric material for combined elastocaloric/electrocaloric refrigeration. In the tests performed the electric field varies in 0÷100 MV/m, whereas the stress field changes in 0÷2 GPa range; the cycle frequency is 1.25 Hz, selected since it optimizes the cycle performances; whereas three different fluid flow rate have been tested (0.034, 0.046, 0.057 kg/s). The tests have been carried out the T_C÷T_H temperature range of 292÷300 K.

The energy performances of the caloric refrigerator in the a), b) and c) cases have been investigated in terms of temperature span (ΔT_{span}), cooling power and Coefficient Of Performance (COP). The ΔT_{span}, obtained by evaluating the difference between T_H and the cold side temperature of the secondary fluid averaged in the last process of the AER/AeR/multicaloric cycle (fluid flowing from hot to cold side of the regenerator), is evaluated as in the following equation:

$$\Delta T_{span} = T_H - \int_{3\tau}^{4\tau} T_f(0,y,t)\,dt \tag{10}$$

The cooling power and the power related to the heat supplied in the environment are calculated as:

$$\dot{Q}_{ref} = \frac{1}{4\tau}\int_{3\tau}^{4\tau} \dot{m}_f C_f\big(T_C - T_f(0,y,t)\big)\,dt \tag{11}$$

$$\dot{Q}_{rej} = \frac{1}{4\tau}\int_{\tau}^{2\tau} \dot{m}_f C_f\big(T_f(L,y,t) - T_H\big)\,dt \tag{12}$$

The mechanical power associated with the circulation pump is:

$$\dot{W}_p = \frac{\dot{m}(\Delta p_{CF} + \Delta p_{HF})}{\eta_p \rho_f}(t_{CF} + t_{HF}) \tag{13}$$

The Coefficient of Performance has been introduced to estimate the performance of the two models as follows:

$$COP = \frac{\dot{Q}_{ref}}{\dot{Q}_H - \dot{Q}_{ref} + \dot{W}_p} \tag{14}$$

5. Results

Several AER/AeR cycles have been performed to make the proposed comparison among the electrocaloric, elastocaloric and combined multicaloric behavior of $PbTiO_3$, in terms of energetic performances, when it is employed as refrigerant in a solid-state cooler. Fig.2 reports ΔT_{span}, detected in a) b) and c) cases, under the three fluid-flow rate investigated in the temperature range of 292÷300 K. One can observe that the temperature span is larger as smaller is the water mass flow rate; to this reason, a regeneration of the fluid allows touching smaller temperatures proper on the cold side. When $PbTiO_3$ is employed as elastocaloric refrigerant, on equal operative condition, it confers higher ΔT_{span} rather than it plays the role of electrocaloric solid-state material. As a matter of fact, if the two effects are combined, ΔT_{span} values increase around +23% with respect to electrocaloric case and +16% to elastocaloric one. Figure 3 displays the cooling power Q'_{ref}, detected in a) b) and c) cases, under the three fluid-flow rate investigated in the temperature range of 292÷300 K. The refrigerating power is higher as long as the greater is the water flow rate. Cooling powers related to $PbTiO_3$ as electrocaloric or elastocaloric refrigerant, lead to values at least of 125 W and 170 W, respectively. A combined multicaloric employment of $PbTiO_3$ in a solid-state refrigerator carries to higher cooling powers, with a medium increment of +70%, with a maximum of +75%, when for fluid-flow rate of 0.057 kg/s, the refrigerating power registered is 292 W. Figure 4 illustrates the Coefficient of Performance (COP) evaluated for $PbTiO_3$ in the three cases presented in this work, by varying fluid flow rate. As the refrigerant power, also COP increases according to the increase of the water flow rate.

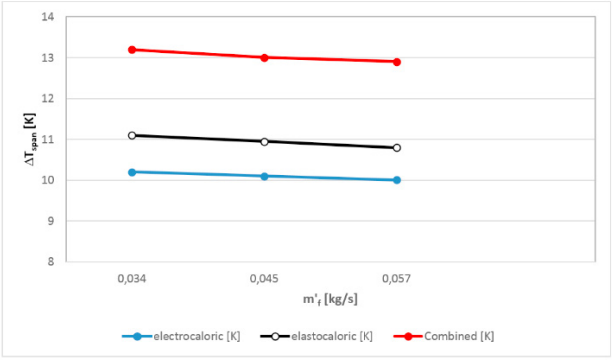

Fig. 2. ΔT_{span} vs m'_f in AER, AeR and multicaloric solid-state regenerator.

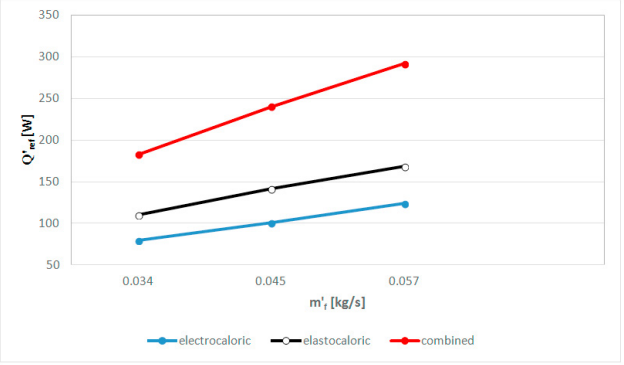

Fig. 3. Q'_{ref} vs m'_f in AER, AeR and multicaloric solid-state regenerator.

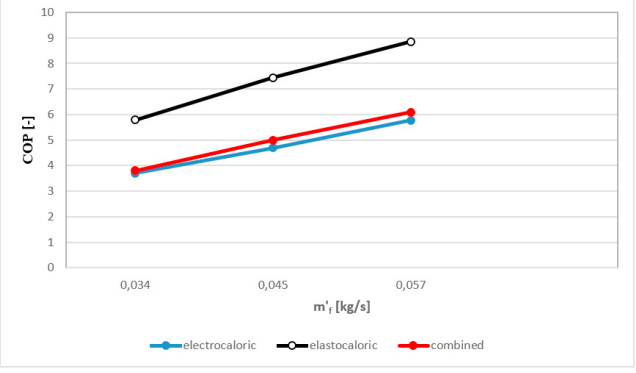

Fig. 4. *COP* vs m'_f in AER, AeR and multicaloric solid-state regenerator.

As a matter of fact, the cooling power registered in the electrocaloric case is lower than elastocaloric one and the expense associate to electrical power is greater than the mechanical power required for stress applying in the elastocaloric case The COPs registered for combined effect are not so high because the double expense associated both with electrical and mechanical power to apply simultaneously electric field and stress to the refrigerant cuts down significantly the great benefits carried by so higher cooling power registered, thus resulting in smaller values of COP than expected. From figure 4 one can deduce that the highest COPs are registered when $PbTiO_3$ is employed as elastocaloric refrigerant, with a maximum value (8.9) obtained with fluid flow rate of 0.057 kg/s.

6. Conclusion

In this paper is introduced an experimental investigation conducted on a two-dimensional model of solid-state cooler when it employs $PbTiO_3$, a multicaloric material which presents both electrocaloric and elastocaloric effect, in order to explore its energetic performances both when the material only shows electrocaloric or elastocaloric effect alone and when its multicaloric nature takes place. The energetic performances have been evaluated in terms of temperature span, cooling power and coefficient of performance, while $PbTiO_3$ was employed as a) electrocaloric, b) elastocaloric, c) multicaloric refrigerant in a solid-state refrigerator mounting an active caloric regenerator. The performances have been evaluated for a number of fluid-flow rates, whereas both the frequency and the cold and hot heat exchanger temperatures have been kept constant. The results reveal that $PbTiO_3$ as elastocaloric refrigerant confers the best performances in terms of COP: one of the reason lies in the lowest expense registered for applying field variation. On the other side, the highest cooling power estimated are proper of combined elastocaloric-electrocaloric effect, with increments around +65% than employing $PbTiO_3$ in single electrocaloric/elastocaloric refrigeration, on equal operative conditions.

References

[1] Montreal Protocol on substances that deplete the ozone layer. United Nation Environment Program (UN), New York (NY), USA, 1987.
[2] Aprea C, Greco A, Maiorino A. "The substitution of R134a with R744: an exergetic analysis based on experimental data." *Int. J. of Refri.* 2013; 36:2148-2159.
[3] Kyoto Protocol to the United Nation Framework Convention on climate change. United Nation Environment Program (UN), Kyoto, JPN, 1997.
[4] Aprea C, Greco A, Maiorino A, Masselli C, Metallo A. "HFO1234yf as a drop-in replacement for R134a in Domestic Refrigerators: A life cycle climate performance analysis." *Int. J. of Heat and Techn.* 2016; 34.S2:S212-S218.
[5] Greco A, Mastrullo R, Palombo A. "R407C as an alternative to R22 in vapour compression plant: An experimental study" *Int. J. of En. Res.* 1997; 71.12:1087-1098.
[6] Vallati A, Grignaffini S, Romagna M, Mauri L, Energy retrofit of a non-residential and historic building in Rome. Environment and Electrical Engineering (EEEIC). IEEE 16th International Conference on Environment and Electrical Engineering 2016.
[7] Mauri L. "Feasibility Analysis of Retrofit Strategies for the Achievement of NZEB Target on a Historic Building for Tertiary Use." *Energy Procedia* 2016; 101:1127-1134.
[8] Mauri L, Carnielo E, Basilicata C. "Assessment of the impact of a centralized heating system equipped with programmable thermostatic valves on building energy demand." *Energy Procedia* 2016; 101:1042-1049.
[9] Salata F, Golasi I, Falanga G, Allegri M, De Lieto Vollaro E, Nardecchia F, Pagliaro F, Gugliermetti F, De Lieto Vollaro A. "Maintenance and energy optimization of lighting systems for the improvement of historic buildings: A case study". *Sustainability (Switzerland)* 2015; 7.8:10770-10788.
[10] Fichera A, Frasca M, Volpe R. "Complex networks for the integration of distributed energy systems in urban areas". *Applied Energy* 2017; 193:336-345.
[11] Lo Cascio E, Borelli D, Devia F, Schenone C. "Future distributed generation: An operational multi-objective optimization model for integrated small scale urban electrical, thermal and gas grids". *Energy Conversion and Management* 2017; 143:348-359.
[12] Ozbolt M, Kitanovski A, Tusek J, Poredos T. "Electrocaloric refrigeration: Thermodynamics, stat of the art and future perspectives." *Int. J. of Refrig.* 2014; 40:174-188.
[13] Aprea C, Greco A, Maiorino A, Masselli C. "A comparison between electrocaloric and magnetocaloric materials for solid state refrigeration", *Int. J. of Heat and Techn.* 2017; 35.1:225-234.
[14] Kitanovski A, Plaznik U, Tomc U, Poredos A. "Present and future refrigeration and heat pump technologies." *Int. J. of Refrig.* 2015; 57:288-298.
[15] Aprea C, Greco A, Maiorino A, Masselli C. "Electrocaloric refrigeration: an innovative, emerging, eco-friendly refrigeration technique", IOP Conf. Series: *Journal of Physics: Conf. Series* 2017; 796:012019.
[16] Moya X, Kar-Narayan S, Mathur N D. "Caloric materials near ferroic phase transitions." *Nature materials* 2014; 34.5:1484-1491.
[17] Mañosa L, Planes A, Acet M. "Advanced materials for solid-state refrigeration." *Journal of Materials Chemistry A* 2013; 1.16:4925-4936.
[18] Lisenkov S, Mani B K, Chang C M, Almand J, Ponomareva I. "Multicaloric effect in ferroelectric PbTiO 3 from first principles." *Physical Review B* 2013; 87.22: 224101.
[19] Aprea C, Greco A, Maiorino A, Masselli C. "A comparison between different materials in an active electrocaloric regenerative cycle with a 2D numerical model." *Int. J. of Refrig.* 2016; 69:369-382.